Quantum Information and Computation, Vol. 20, No. 5&6 (2020) 0375–0399

PERSISTENT HOMOLOGY ANALYSIS OF MULTIQUBIT ENTANGLEMENT

RICARDO MENGONI[a]
Dipartimento di Informatica, Università di Verona
Strada Le Grazie 15, 37134 Verona, Italy

ALESSANDRA DI PIERRO[b]
Dipartimento di Informatica, Università di Verona
Strada Le Grazie 15, 37134 Verona, Italy

LELEH MEMARZADEH[c]
Department of Physics, Sharif University of Technology, Tehran, Iran

STEFANO MANCINI[d]
School of Science and Technology, University of Camerino, I-62032 Camerino, Italy
and
INFN Sezione di Perugia, I-06123 Perugia, Italy

Received December 23, 2019
Revised March 16, 2020

We introduce a homology-based technique for the classification of multiqubit state vectors with genuine entanglement. In our approach, we associate state vectors to data sets by introducing a metric-like measure in terms of bipartite entanglement, and investigate the persistence of homologies at different scales. This leads to a novel classification of multiqubit entanglement. The relative occurrence frequency of various classes of entangled states is also shown.

Keywords: Entanglement Classification, Persistent Homology
Communicated by: R Jozsa & J Eisert

1 Introduction

Entanglement has been recognized as a key resource for obtaining a quantum boost in many information technology tasks (see e.g. [1]). As such it deserves a careful characterization. In fact it is important to know which states can perform the same tasks equally well. Initial work on the classification of entangled states was focused on the quantification through so-called 'entanglement monotones', i.e. functions of multipartite states that do not increase under local transformations [2]. Most of these functions work only for bipartite systems [3], although some examples for multipartite systems have also been devised (see e.g. [6]). There, another approach seems to be more promising, which is based on partitioning states according

[a]riccardo.mengoni@univr.it
[b]alessandra.dipierro@univr.it
[c]memarzadeh@sharif.edu
[d]stefano.mancini@unicam.it

to some notion of equivalence. Noticeable are equivalence classes constructed on the basis of invariance under Stochastic Local Operations and Classical Communication (SLOCC) [4]. However, this leads to infinite (even uncountable) classes for more than three qubit systems. Hence this approach is not effective in the general case, although some ways out were devised for the case of four qubits [5].

An alternative route to entanglement classification is represented by the analysis of topological features of multipartite quantum states [7, 8]. Topological data analysis has recently gained a lot of attention in the classical framework thanks to its suitability for the analysis of huge data sets represented in the form of point clouds: in such cases, it would indeed be impossible to accurately analyze the data, while a "qualitative" analysis would be efficient. Among these techniques, Persistent Homologies (PH) plays a pivotal role [9, 10]. This is a particular sampling-based technique from algebraic topology aiming at extracting topological information from high-dimensional data sets.

In this paper, following up the work in [8], we apply PH techniques to analyse multiqubit state vectors. Each state vector will be intended as a data set on which a metric-like measure is defined in terms of bipartite entanglement. More specifically, given a vector state of N qubits we consider N points each one representing a qubit and then arrange them in such a way that their pairwise distance is inversely proportional to the two-points correlation. Then, bar code [9,10] is constructed for this data set. Two states are in the same class if they have the same bar codes. Actually, the exact position of a bar in the bar code is not relevant for our purpose, only its presence or absence is essential. While the aim of [8] is the classification of all possible states for 3 and 4 qubit, here we focus on genuine entanglement and show the classification up to 6 qubit. Moreover, in this paper we will also compute the relative occurrence frequency of the various classes of genuine entangled states, by means of a random generation of states.

The article is organized as follow. In Section 2 we briefly recall concepts of algebraic topology that will be used thereafter. In Section 3 we illustrate the method to produce a data cloud from multiqubit states. Then, in section 4, we produce and show the barcodes for the cases of 4 and 5 qubit. (those for 6 qubit are reported in the Appendix). We also analyze the occurrence frequency of various classes of genuine entangled states. Finally, we draw our conclusions in Section 5.

2 Persistent Homology

A data cloud is a collection of points in some n-dimensional space $\mathbb{S}_n$. In many cases, analysing the global 'shape' of the point cloud gives essential insights about the problem it represents. In the context of data analysis, Persistent Homology is an algebraic method for computing coarse topological features of a given data cloud that persist over many grouping scales. In this section we review the mathematical background that is necessary to understand this technique [11, 12].

Consider a data cloud represented by a set of points $\{x_\alpha\}$ living in a Euclidean space. Choosing a value of the grouping scale ϵ, it is possible to construct the graph whose vertices are the data points $\{x_\alpha\}$ and edges $e_{x_\alpha, x_{\alpha'}}$ are drawn when the $\frac{\epsilon}{2}$-balls centered in the vertices x_α and $x_{\alpha'}$ intersect each other. Such graphs show connected components and hence clusters obtained at ϵ scale but do not provide information about higher-order features such as holes

and voids. In order to track high-dimensional features we need to introduce the following concepts.

Convex set. A convex set is a region of a Euclidean space where every two points can be connected by a straight line segment that is also within the region.

Convex Hull. The convex hull of a set X of points in an Euclidean space is the smallest convex set that contains X.

k-Simplex. A k-simplex is a k-dimensional polytope which is the convex hull of its $k+1$ vertices. Thus, for example, simplices of dimension $0, 1, 2$ and 3 are respectively vertices, edges, triangles and tetrahedra. A face of a k-simplex is the convex hull of any non empty subset of its $k+1$ vertices.

Simplicial Complex. A simplicial complex $\mathcal{K}$ is a set of simplices that satisfies the conditions:

i) Any face of a simplex from $\mathcal{K}$ is also in $\mathcal{K}$.

ii) The intersection of any two simplices $\sigma_1, \sigma_2 \in \mathcal{K}$ is either an empty set or a face of both σ_1 and σ_2.

The dimension of a simplicial complex is equal to the largest dimension of its simplices.

Homology of a complex. For each simplicial complex $\mathcal{K}$ there is a set of homological groups $\{H_0(\mathcal{K}), H_1(\mathcal{K}), H_2(\mathcal{K}), \ldots\}$, where the kth homology group $H_k(\mathcal{K})$ is non-empty when the k-dimensional holes are in $\mathcal{K}$. Hence, the homological groups of the simplicial complex describe the order of the holes existing in that simplicial complex.

In order to recognize global topological features of a data cloud it is necessary to complete the corresponding graph to a simplicial complex by filling in the graph with all the simplices. Given a grouping scale ϵ, there are different methods to generate simplicial complexes. In this paper we will focus on the Rips complex, $\mathcal{R}_\epsilon$, where k-simplices correspond to $(k+1)$ points which are pairwise within distance ϵ.

Topological features of the data cloud are obtained by constructing a homology of the simplicial complex. The homology of the Rips complex hence reveals those topological features that appear at a chosen value of ϵ. If ϵ is taken too small, then only multiple connected components are shown. On the other hand, when ϵ is large, any pairs of points get connected and a giant simplex with trivial homology is obtained. However, it is preferable to make the whole process independent from the choice of ϵ. In order to obtain significant features it is necessary to consider all the range of ϵ. Those topological features which persist over a significant interval of the parameter ϵ are to be considered specific of that point cloud, while short-lived features as less important ones. Consider the sequence of Rips complexes $\mathsf{R} = \{\mathcal{R}_{\epsilon_i}\}_{i=1}^N$ associated to a given point cloud; instead of examining the homology $H(\mathcal{R}_{\epsilon_i})$ of the individual terms, we look at the inclusion maps $I : H(\mathcal{R}_{\epsilon_i}) \to H(\mathcal{R}_{\epsilon_j})$ for all $i < j$. These maps are able to tell us which features persist since they reveal information that is not visible if we consider $H(\mathcal{R}_{\epsilon_i})$ and $H(\mathcal{R}_{\epsilon_j})$ separately.

Barcodes. Given the sequence of Rips complexes $\mathsf{R} = \{\mathcal{R}_{\epsilon_i}\}_{i=1}^N$, a *barcode* is a graphical representation of $H_k(\mathsf{R})$ as a collection of horizontal line segments in a plane whose horizontal

axis corresponds to the parameter ϵ and whose vertical axis represents an (arbitrary) ordering of homology groups. A barcode can be seen as a variation over ϵ of the Betti numbers which count the number of n-dimensional holes on a simplicial complex $\mathcal{R}_\epsilon$ (cf. [13]).

3 Creating qubit data cloud

In this section we discuss the methodology we use for creating the data cloud which will be at the basis of classifying entangled states. We will restrict our attention to N qubit states showing "genuine" entanglement, i.e. that are N-partite entangled or "fully inseparable".

Our approach starts with the random generation of pure states among which we select, using generalised concurrence measure, those showing genuine entanglement. At this stage, a data cloud is associated to a state in such a way that each qubit is identified with a single point in the cloud, while a distance between pairs of points is defined using a semi-metric that takes into account the pairwise entanglement shared by the two qubits that the points represent. Semi-distances between qubits are stored in a matrix D which will be the input of the persistent homology algorithm.

Note that in the definitions given in Section 2 we refer for simplicity to Euclidean spaces. Since here we are dealing instead with a semi-metric space, it is worth noting that computing persistent homology is still possible in our case. In fact, a distance between pairs of points which does not satisfy triangular inequality is still sufficient for constructing Rips complexes.

3.1 Random state generation

In order to randomly generate a pure state of N qubits, we employ the following parametrization [14, 15]

$$|\psi\rangle = \sum_{n=0}^{2^N-1} \nu_n |n\rangle, \tag{1}$$

with

$$\nu_0 = \cos\theta_{2^N-1}, \tag{2}$$

$$\nu_{n>0} = e^{i\phi_n} \cos\theta_{2^N-1-n} \prod_{l=2^N-n}^{2^N-1} \sin\theta_l. \tag{3}$$

and

$$\theta_n := \arcsin\left(\xi_n^{\frac{1}{2n}}\right). \tag{4}$$

The independent random variables $\phi_{n\geq 1}$ and $\xi_{n\geq 0}$ are uniformly distributed in the intervals:

$$\phi_{n\geq 1} \in [0, 2\pi), \qquad \xi_n \in [0, 1].$$

3.2 Entangled states selection

After generating a random N-qubit state $|\psi\rangle$ we check that it is actually N-partite entangled. This happens iff for every bipartition $A/\hat{A}$ (where $\hat{A}$ denotes the complement set of A) of the N-qubit, $\mathcal{C}_G(\rho_A) \neq 0$, where $\mathcal{C}_G$ is the generalized concurrence defined in [16] as follows:

$$\mathcal{C}_G(\rho_A) := 2\sqrt{1 - \mathrm{Tr}(\rho_A^2)}. \tag{5}$$

3.3 Distances calculation

It is possible to generate barcodes for simplicial complexes corresponding to a points (i.e. qubits) cloud by giving in input to the persistent homology algorithm the matrix D of all pairwise distances between points.
In [8], a semi-distance $1/E_{i,j}$, was proposed, where $E_{i,j}$ is an entanglement monotone calculated between qubit i and qubit j. This semi-distance goes from 1 (when the two qubit are maximally entangled) to $+\infty$ (when they are separable). Here we use the following semi-metric:

$$D_{i,j} = 1 - \exp\left\{1 - \frac{1}{C_{i,j}}\right\}, \tag{6}$$

where $C_{i,j}$ is the concurrence between qubit i and qubit j. The semi-distance $D_{i,j}$ goes from 0 to 1 as the entanglement decreases, and remains finite for separable states. The choice of this semi-metric reflects the fact that we intuitively consider two points closer if they are more correlated, while farthest if they are less correlated.

Recall that, given a state ρ on N qubits, the concurrence between two qubits i and j is obtained by first tracing out all other $N-2$ qubits. This gives the reduced density matrix ρ_{ij}. Then

$$C_{i,j} := \max\{0, \lambda_1 - \lambda_2 - \lambda_3 - \lambda_4\}, \tag{7}$$

where $\lambda_1, \lambda_2, \lambda_3, \lambda_4$, are the square root of the eigenvalues (in decreasing order) of the matrix $\rho_{ij}(\sigma_y \otimes \sigma_y)\rho^*_{ij}(\sigma_y \otimes \sigma_y)$ [17], with σ_y the well known Pauli matrix and ρ^*_{ij} the complex conjugate of $\rho_{i,j}$ in the computational basis.

4 Entanglement classification

We have used the TDA package for computing persistent homology and barcodes developed for the *R software* [18]. The classification is obtained by grouping together those states with the same barcode. This is done without caring about the position of a bar, but only to its presence or absence.

In the following barcodes, black lines represent connected components (i.e. homology group H_0), red lines represent holes (i.e. homology group H_1) and blue lines represent voids (i.e. homology group H_2). All barcodes are generated using the Rips complex.

4.1 Classification of four qubits states

Barcodes generated by 4-partite entangled states of 4 qubits and relative frequencies are shown starting from the most frequent to the least frequent one.

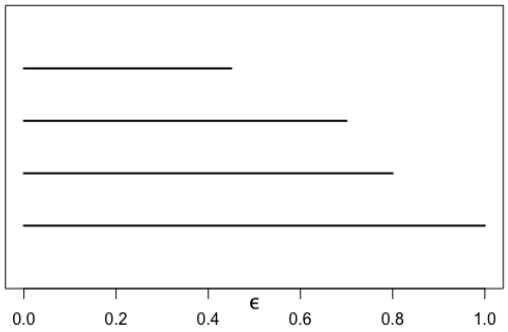

Fig. 1. Barcode of the class labelled as **4B1**.

Genuine entangled states with the barcode shown in Figure 1 have a total of four connected components: three of them end at value of $\epsilon < 1$, while only one component persists over all the range of ϵ. The fact that only one connected component persists means that the state form a single cluster of qubits grouped by pairwise entanglement without showing higher homological features. A representative of such class is the $|W\rangle$ state.

$$|4, B1\rangle \equiv |W\rangle_4 = \frac{1}{2}(|0001\rangle + |0010\rangle + |0100\rangle + |1000\rangle)$$

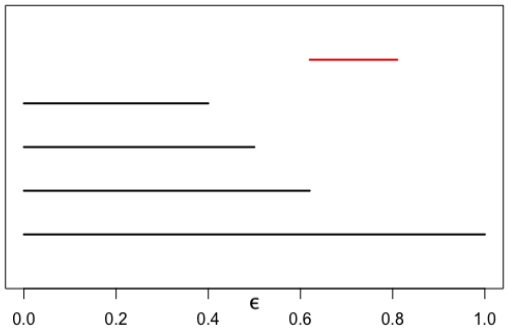

Fig. 2. Barcode of the class labelled as **4B2**.

States belonging to class of Figure 2 form again a single persistent component of pairwise entanglement between qubits. However in this case a hole, denoted by the red bar H_1, appears when only one connected component is left. Such a hole has limited life-span since disappears when ϵ is sufficiently large. A state showing such a behaviour is the following:

$$|4, B2\rangle = \frac{1}{2\sqrt{2}}\left(\sqrt{2}|0000\rangle + |0011\rangle + |0110\rangle + |1001\rangle + |1100\rangle + \sqrt{2}|1111\rangle\right)$$

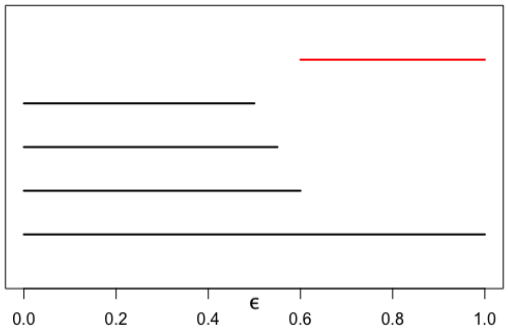

Fig. 3. Barcode of the class labelled as **4B3**.

In the case shown in Figure 3, a single connected component is left and a persistent hole is present. States with this barcode have the characteristic that each qubit is pairwise entangled to other two qubits and completely un-entangled with a third qubit. A state showing such properties is

$$|4, B3\rangle = \frac{1}{2}\left(|0000\rangle + |0011\rangle + |1010\rangle + |1111\rangle\right)$$

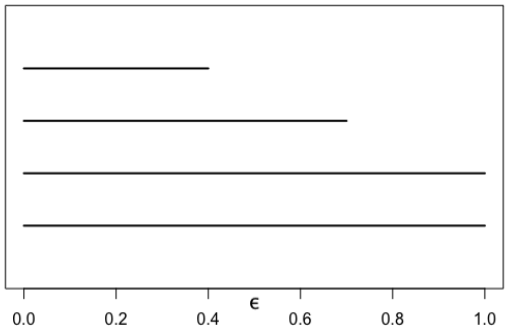

Fig. 4. Barcode of the class labelled as **4B4**.

In the class represented by the barcode in Figure 4 we find genuinely entangled states with no higher homological feature than H_0 which have two different connected component that persist over the range of ϵ. This means that such states have two sets of qubits which are internally connected by pairwise entanglement to form a component, but no connection is present among qubits of different sets. Yet a single qubit in a set could be entangled to the other set as a whole. An example for this class is the state:

$$|4, B4\rangle = \frac{1}{2}\left(|0011\rangle + |1011\rangle + |1101\rangle + |1110\rangle\right)$$

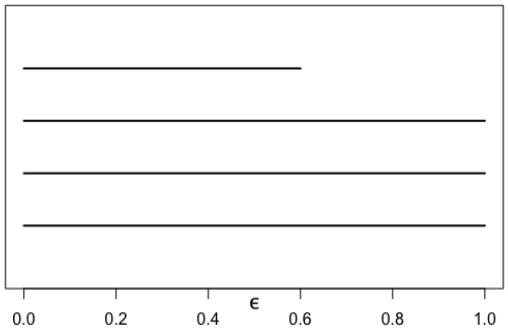

Fig. 5. Barcode of the class labelled as **4B5**.

Like the previous case, states with the barcode of Figure 5 only show four connected components, three of which persist while one has limited lifetime. The characteristic of these states is that there are always 2 qubits which do not share any pairwise entanglement with another qubit, while the other two do. A representative state for this class is

$$|4, B5\rangle = \frac{1}{\sqrt{3}} \left(|0000\rangle + |0111\rangle + |1101\rangle\right)$$

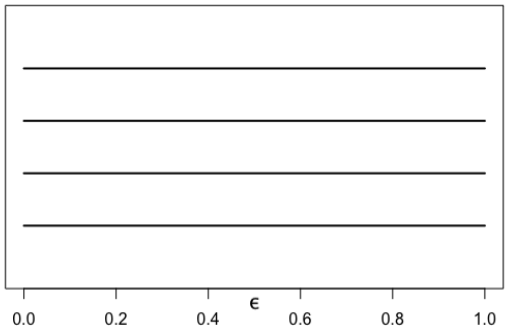

Fig. 6. Barcode of the class labelled as **4B6**.

States of the kind shown in Figure 6 do not have any pairwise entanglement among qubits. For this reason no qubit get connected to another and we see four distinct components that persist. A representative of this class is the $|\mathrm{GHZ}\rangle$ state.

$$|4, B6\rangle \equiv |\mathrm{GHZ}\rangle_4 = \frac{1}{\sqrt{2}}(|0000\rangle + |1111\rangle)$$

As we can observe in Fig.7, there exist six different classes of four qubit genuine entangled states, based on the persistent homology classification. The most frequent class (61.70%) is the one where only one component persists (**4B1**), states like W belong to to this class. With frequencies of 17.31% and 10.60% we find states with barcodes **4B2** and **4B3** showing

one persistent connected component and a hole (red line) that in the case of **4B3** is also persistent. The last three barcodes, in order **4B4**, **4B5** and **4B6** show an increasing number of disconnected components. States that are GHZ-like are hence the least frequent (0.52%).

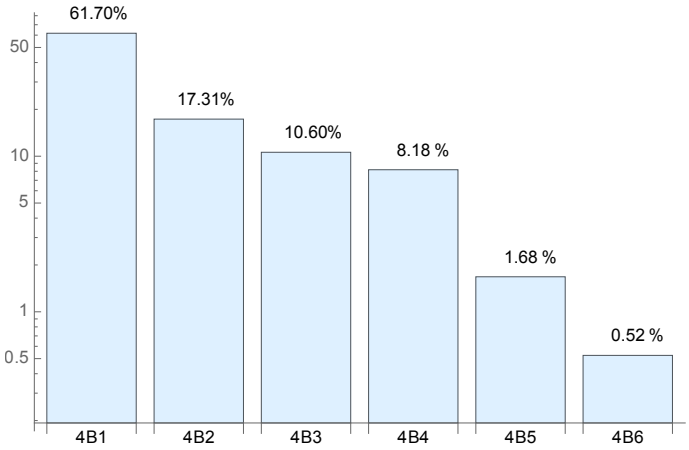

Fig. 7. Barcode frequencies (in Log scale) for four qubits genuine entangled states.

4.2 Classification of five qubits states

Let's now consider randomly generated 5-partite entangled states of 5 qubits. Barcodes and relative frequencies are shown below starting from the barcode more likely to appear to the least frequent one

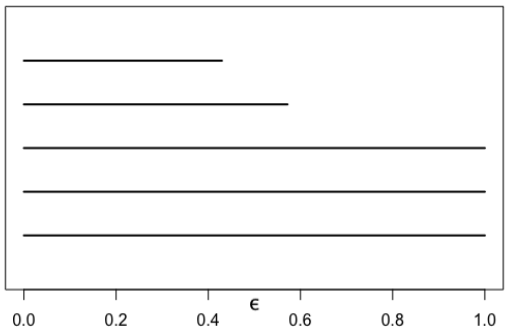

Fig. 8. Barcode of the class labelled as **5B1**.

In the five qubit case, the most frequent class shows a barcode like the one in Figure 8 with three connected components that persist in the range of D. States of this kind have at least one qubit (up to two qubits) that does not share pairwise entanglement with any other qubit. This configuration does not generate higher homology groups than H_0. An example of state in this class is

$$|5, B1\rangle = \frac{1}{\sqrt{5}} \left(|00001\rangle + |00011\rangle + |00110\rangle + |01000\rangle + |11011\rangle \right)$$

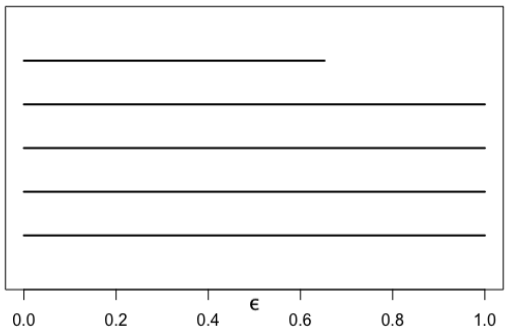

Fig. 9. Barcode of the class labelled as **5B2**.

As we can see, the barcode of Figure 9 shows four persistent connected components i.e. only two qubits among five share pairwise entanglement while all remaining qubits act as independent connected component. A representative state for this class is

$$|5, B2\rangle = \frac{1}{\sqrt{5}} \left(|00001\rangle + |00011\rangle + |00100\rangle + |01100\rangle + |11010\rangle\right) \tag{8}$$

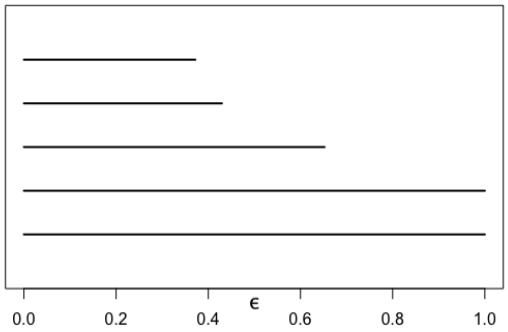

Fig. 10. Barcode of the class labelled as **5B3**.

In this class identified by the barcode of Figure 10, two connected components persist while the other three have limited lifetime. Two clusters of qubits connected by pairwise entanglement are hence created and no holes or higher topological features appear. An example of state in this class is the following

$$|5, B3\rangle = \frac{1}{\sqrt{5}} \left(|00001\rangle + |00010\rangle + |00100\rangle + |01000\rangle + |10111\rangle\right)$$

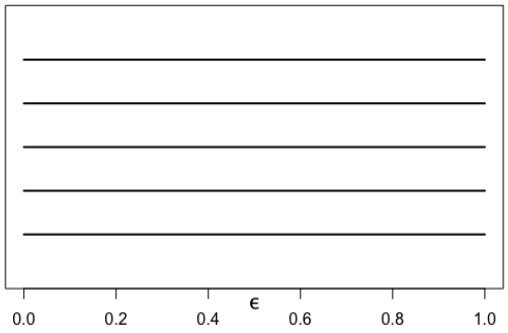

Fig. 11. Barcode of the class labelled as **5B4**.

Figure 11 show the barcode of the class where we find GHZ like states, i.e. those states where there are no entangled pair of qubits and hence show five persistent connected components in the barcode.

$$|5, B4\rangle \equiv |\mathrm{GHZ}\rangle_5 = \frac{1}{\sqrt{2}} \left(|00000\rangle + |11111\rangle\right)$$

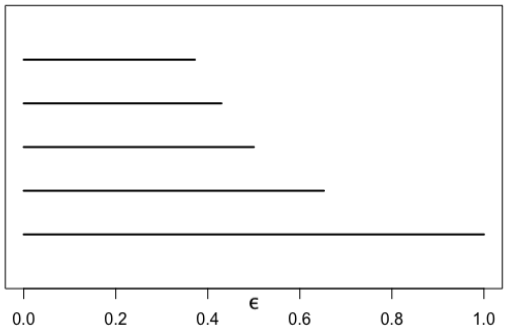

Fig. 12. Barcode of the class labelled as **5B5**.

After we find the barcode shown in Figure 12 and relative to those states like $|W\rangle$ which have only one connected component and hence pairwise entanglement creates a single cluster of qubits.

$$|5, B5\rangle \equiv |\mathrm{W}\rangle_5 = \frac{1}{\sqrt{5}} \left(|00001\rangle + |00010\rangle + |00100\rangle + |01000\rangle + |10000\rangle\right)$$

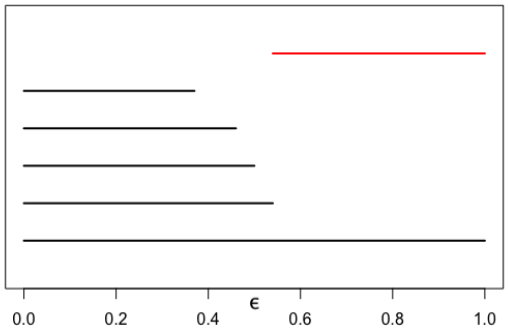

Fig. 13. Barcode of the class labelled as **5B6**.

Figure 13 shows the barcode of the first class of 5 qubits genuinely entangled states that present a first order homology group H_1, i.e. a hole, in the barcode. States in this class have their qubits connected to form a single persistent component when $\epsilon \approx 1$. Note also that some subsets of qubits do not share any pairwise entanglement and hence are responsible for the persistent hole. An example of state in this class is

$$|5, B6\rangle = \frac{1}{\sqrt{6}} \left(|00000\rangle + |11000\rangle + |01100\rangle + |00110\rangle + |00011\rangle + |10001\rangle\right)$$

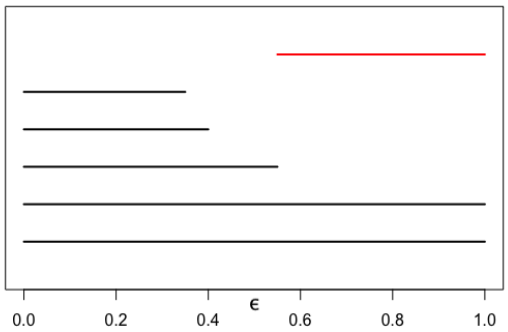

Fig. 14. Barcode of the class labelled as **5B7**.

As we can see in Figure 14, like in the previous class, a hole is created at some value of ϵ and persists up to the upper limit of the semi-metric D. However here while four qubits are responsible for one connected component and for the H_1 homology, the remaining fifth qubit does not share any pairwise entanglement with the others and creates a persistent component on its own. A representative state of this kind is

$$|5, B7\rangle = \frac{1}{\sqrt{5}} \left(|00010\rangle + |00011\rangle + |00101\rangle + |10111\rangle + |11011\rangle\right)$$

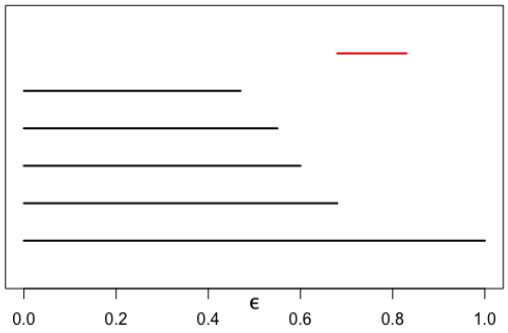

Fig. 15. Barcode of the class labelled as **5B8**.

States in the class of Fig.15 have similar properties to those in the class of Fig.13, however in this case the H_1 homology does not persist since connections among qubits creating the hole appear at some value of ϵ. An example state with such barcode could be

$$|5, B8\rangle = \frac{1}{\sqrt{10}}\left(\sqrt{5}|00000\rangle + |11000\rangle + |01100\rangle + |00110\rangle + |00011\rangle + |10001\rangle\right). \quad (9)$$

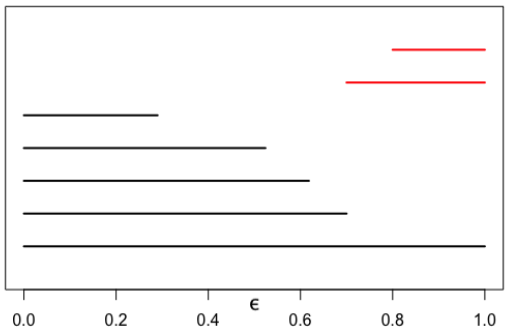

Fig. 16. Barcode of the class labelled as **5B9**.

The class characterized by the barcode depicted in Figure 16 shows a single persistent connected component of qubits grouped by pairwise entanglement but also two holes which appear at some ϵ and persist for higher values. A representative for this class is the following

$$|5, B9\rangle = \sqrt{\frac{2}{5}}\left(|00000\rangle + |01010\rangle\right) + \frac{1}{5}\left(|00011\rangle + |00101\rangle + |01100\rangle + |11000\rangle + |10001\rangle\right)$$

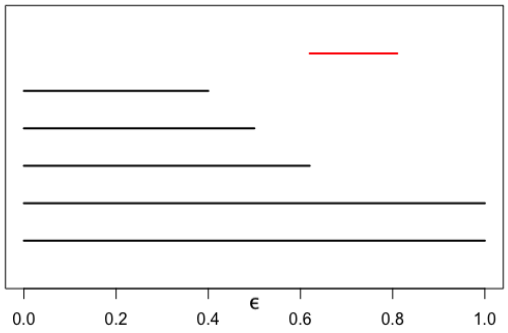

Fig. 17. Barcode of the class labelled as **5B10**.

States belonging to the class of Figure 17 have similar properties to those in class with barcode in Figure 14, i.e. two persistent connected components, one of which is made up of a single qubit which does not share pairwise entanglement with the other four. In the other instead, the remaining four qubits get connected to form a non-persistent hole. An example state with such barcode could be

$$|5, B10\rangle = \frac{1}{\sqrt{6}} \left(|01000\rangle + |01010\rangle + |10000\rangle + |10001\rangle + |10110\rangle + |11010\rangle\right)$$

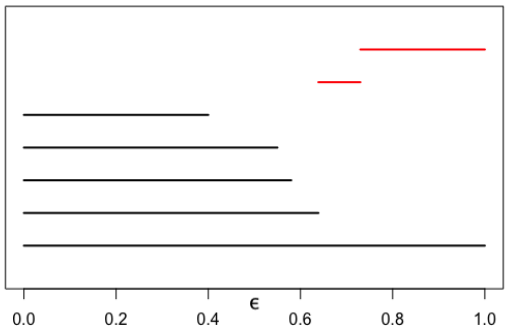

Fig. 18. Barcode of the class labelled as **5B11**.

A single persistent connected component and two holes characterize the barcode of this class, as shown in Figure 18. Note that one of the two homology group generators H_1 appears only in a limited interval while the other one persists over ϵ. An example state with such barcode:

$$|5, B11\rangle = \frac{1}{\sqrt{11}} \left(\sqrt{5}|00010\rangle + \sqrt{2}|00100\rangle + \sqrt{2}|10000\rangle + |10101\rangle + |11100\rangle\right)$$

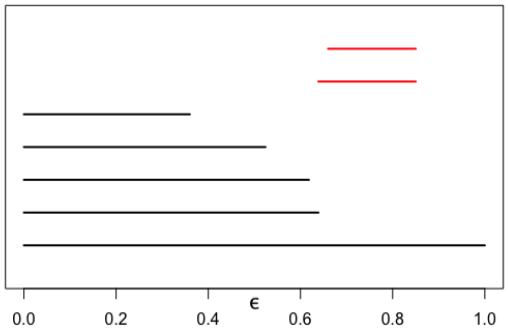

Fig. 19. Barcode of the class labelled as **5B12**.

The least frequent class, barcode in Figure 19, is the one composed of those states where qubits get connected to form a single connected component allowing the presence of two hole that however do not persist. An example state with such barcode is the following

$$|5, B12\rangle = \frac{1}{\sqrt{2}}\,|00000\rangle + \frac{1}{\sqrt{10}}\,(|11000\rangle + |01100\rangle + |01010\rangle + |00101\rangle + |10001\rangle)$$

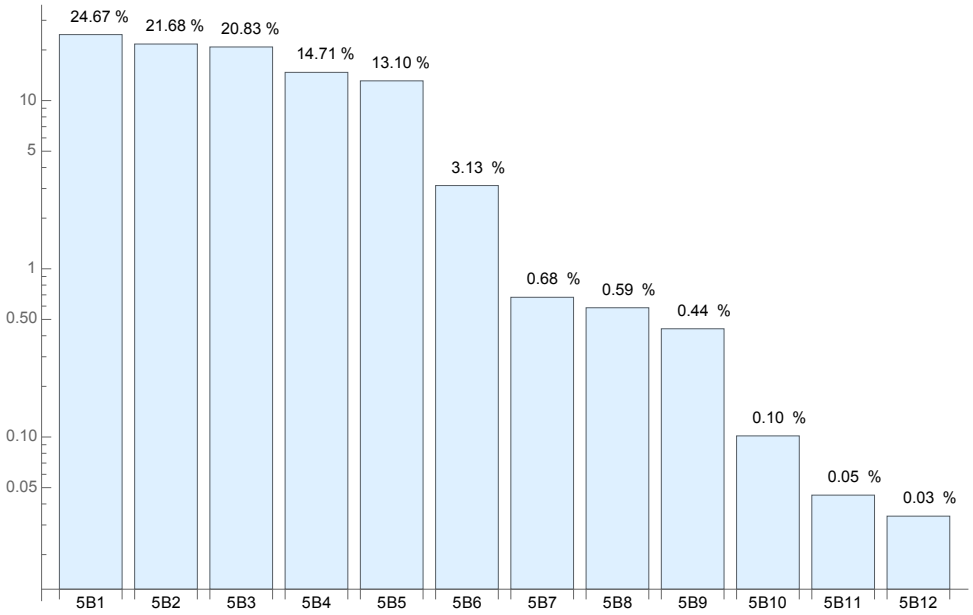

Fig. 20. Barcode frequencies (in Log scale) for five qubits genuine entangled states.

By looking at the chart in Figure 20 it can be noticed that the most frequent barcode (**5B1**) belongs to states with three connected components, followed by states with barcodes showing four, two, five and one persistent components (respectively **5B2**, **5B3**, **5B4**, **5B5**). The 95% of all randomly generated states fall inside one of these first five classes. After them,

barcodes with higher dimensional homology features start to appear: at first those with one hole and then those with two. The only exception is given by barcode **5B10** (showing one short-lived hole but two connected components) since it is less frequent than **5B9** (one connected component and two persistent holes).

4.3 Classification of six qubits states

By randomly generating six-partite genuine entangled states of six qubits, we obtained 33 different classes. Their barcodes are presented in Appendix 1, while frequencies are shown in Figure 21.

With a frequency of 68%, the class defined by barcode **6B1** is by far the most frequent. Such a class consists of GHZ-like states that present six different connected components, i.e. the single qubits with no pairwise entanglement.

As we have seen, for the five qubit case, the first classes in frequency, from **6B1** to **6B6,** are those containing states showing only connected components (H_0 homology group i.e. black bars).

Then states with one hole start to appear, and later those showing two holes, with the exception of barcodes **6B12** and **6B13**.

Finally, barcodes showing multiple holes and voids, from **6B19** to **6B33** are also possible but they do not appear in the histogram since their frequency is very low ($\ll 0.004\%$).

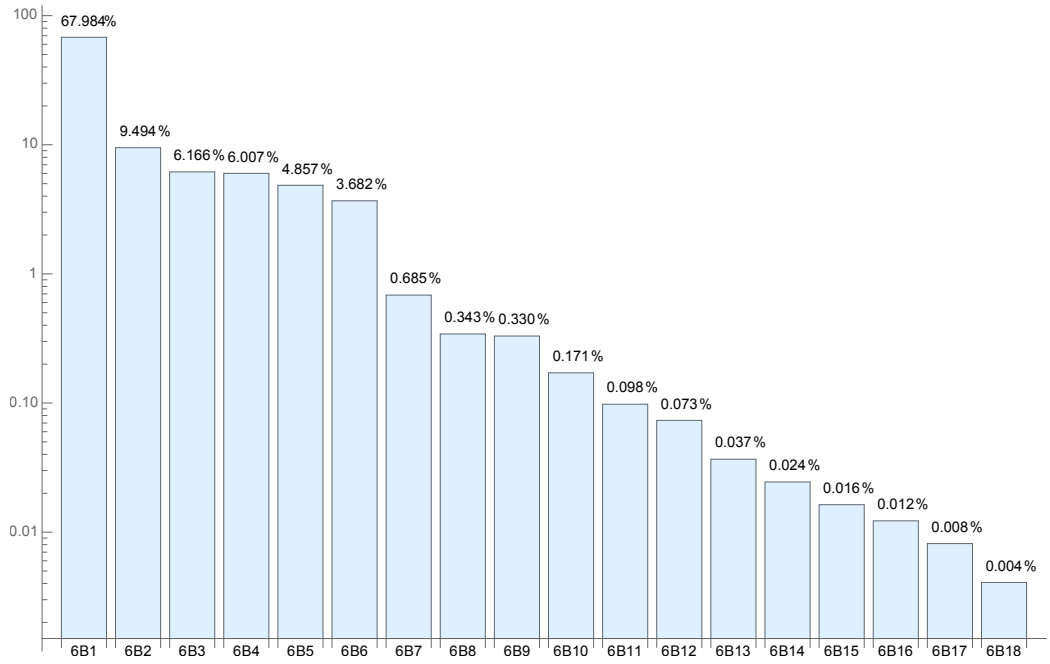

Fig. 21. Barcode frequencies (in Log Scale) for six qubits genuine entangled states.

5 Conclusions

The classification that we have carried out for four, five and six qubits with genuine entanglement shows that it is possible to distinguish respectively six , twelve and thirty-three different classes by persistent homological barcodes.

In general, given a N qubit genuinely entangled state, it is always possible to come up with a finite classification where the total number of possible barcodes B_N is bounded by

$$B_N < \left(\sum_{d=0}^{\frac{N(N-1)}{2}} G_N(d)\ d! \right),$$

where $G_N(d)$ is equal to the number of all possible graphs with N vertices and d edges. The factorial $d!$ is necessary to take into consideration all possible ways of building $G_N(d)$.

Furthermore, patterns seems to emerge in our classifications by looking at the frequencies of barcodes. First of all, those states which are characterized by the only H_0 homology group become more likely as the number of qubits N increases. This is followed by the group of those states showing also H_1 which again are followed by those with a much richer topology. While this fact could be explained from a topological point of view by claiming that, with a limited number of points complex homological patterns in the barcode are harder to obtain, it is still interesting to notice that the same reasoning also hold true for quantum state barcodes.

Among those states with only the H_0 homology group, it is worth noticing that the W-like class, with only one persistent connected component, decreases its frequency with the increase of N. In fact, except for $N = 4$ where we find this class in the first place, in the $N = 5$ and $N = 6$ cases, it falls to the last position. Conversely, the class of states which have N persistent components, like GHZ, gradually increase their frequency, starting from the bottom at $N = 4$ and becoming the most popular at $N = 6$.

In general we can say that increasing the number of qubits makes the randomly generated states easily fall inside classes with more persistent connected components. This seems to indicate that, increasing the number of parties, qubits in a genuine entangled states tend to dislike pairwise entanglement and rather share it with the whole set of other qubits.

The proposed method could be particularly useful to classify eigenstates of solvable Hamiltonians such as [21]. For non-integrable systems, the method can still be applied to approximate eigenstate derived by various techniques such as perturbation theory or numerical analysis. The procedure is to first verify whether or not the eigenstate has genuine multipartite entanglement (as explained in section III.B) and if it is so it is possible to verify the different classes they belong to. It is worth mentioning that if the eigenstates do not have genuine multipartite entanglement, it is still possible to classify them by homological analysis as discussed in [8].

Another consideration is related to the subject of quantum algorithms and their computational complexity classes. As quantum speedup is essentially based on the entanglement employed in the algorithm, it would be interesting to investigate possible relations between quantum computational complexity classes and entanglement classification (see Ref.[19]), based on persistent homology.

Finally,the proposed approach could be easily extendible to mixed states and find applications in the context of open systems dynamics [20].

Acknowledgements

Laleh Memarzadeh would like to acknowledge the support by Sharif University of Technology's Office of Vice President for Research under grant No. G950223.

References

1. M. Walter, D. Gross and J. Eisert (2017), *Multi-partite entanglement*, arXiv:1612.02437.
2. G. Vidal (2000), *Entanglement monotones*, Journal of Modern Optics, **47**, 355.
3. R. Horodecki, P. Horodecki, M. Horodecki and K. Horodecki (2009), *Quantum entanglement*, Reviews of Modern Physics **81**, 865.
4. W. Dur, G. Vidal and J. I. Cirac (2000), *Three qubits can be entangled in two inequivalent ways*, Physical Review A **62**, 062314.
5. F. Verstraete, J. Dehaene, B. De Moor and H. Verschelde (2002), *Four qubits can be entangled in nine different ways* , Physical Review A **65**, 052112;
   Y. Cao, and A. M. Wang (2007), *Discussion of the entanglement classification of a 4-qubit pure state*, European Physical Journal D **44**, 159;
   M. Gharahi and S. J. Akhtarshenas (2016), *Entangled graphs: a classification of four-qubit entanglement*, European Physical Journal D **70**, 54.
6. X. Wang (2002), *Threshold temperature for pairwise and many-particle thermal entanglement in the isotropic Heisenberg model*, Physical Review A **66**, 044305;
   D. Bruß, N. Datta, A. Ekert, L. C. Kwek and C. Macchiavello (2005), *Multipartite entanglement in quantum spin chains*, Physical Review A **72**, 014301;
   T. R. de Oliveira, G. Rigolin, M. C. de Oliveira and E. Miranda (2006), *Multipartite entanglement signature of quantum phase transitions*, Physical Review Letters **97**, 170401;
   S. Campbell and M. Paternostro (2010), *Multipartite nonlocality in a thermalized Ising spin chain*, Physical Review A **82**, 042324;
   H. He and G. Vidal (2015), *Disentangling theorem and monogamy for entanglement negativity*, Physical Review A **91**, 012339;
   A. Bayat (2017), *Scaling of tripartite entanglement at impurity quantum phase transitions*, Physical Review Letters **118**, 036102.
7. G. M. Quinta and A. Rui (2018), *Classifying quantum entanglement through topological links*, Physical Review A **97**, 042307.
8. A. Di Pierro, S. Mancini, L. Memarzadeh and R. Mengoni (2018), *Homological analysis of multiqubit entanglement*, Europhysics Letters **123**, 30006.
9. H. Edelsbrunner, D. Letscher and A. Zomorodian (2002), *Topological persistence and simplification*, Discrete Computational Geometry, **28**, 511.
10. G. Carlsson and A. Zomorodian (2005), *Computing persistent homology*, Discrete Computational Geometry **33**, 249.
11. A. Hatcher (2002), *Algebraic Topology*, Cambridge University Press.
12. H. Edelsbrunner (2014), *A Short Course in Computational Geometry and Topology*, Springer Publishing Company.
13. R. Ghrist (2008), *Barcodes: the persistent topology of data*, Bulletin of the American Mathematical Society **45**, 1.
14. K. Zyczkowski and H. J. Sommers (2001), *Induced measures in the space of mixed quantum states*, Journal of Physics A: Mathematical and General **34**, 35.
15. L. Memarzadeh and S. Mancini (2016), *Minimum output entropy of a non-Gaussian quantum channel*, Physical Review A **94**, 022341.
16. W. K. Wootters (2001), *Entanglement of formation and concurrence*, Quantum Information & Computation **1**, 1.
17. S. Hill and W. K. Wootters (1997), *Entanglement of a pair of quantum bits*, Physical Review Letters **78**, 26.

18. https://CRAN.R-project.org/package=TDA
19. H. Jaffali and F. Holweck, *Quantum entanglement involved in Grover's and Shor's algorithms: the four-qubit case*, arXiv:1811.08894.
20. L. Memarzadeh and S. Mancini (2011), *Stationary entanglement achievable by environment-induced chain links*, Physical Review A **83**, 042329.
21. E. Lieb, T. Schultz and D. Mattis (1961), *Two soluble models of an antiferromagnetic chain*, Annals of Physics **16**, 407;
    S. Katsura (1962), *Statistical mechanics of the anisotropic linear Heisenberg model*, Physical Review **127**, 1508;
    P. Pfeuty (1970), *The one-dimensional Ising model with a transverse field*, Annals of Physics **59**, 79;
    E. Barouch and B. McCoy (1971), *Statistical Mechanics of the XY model. II. Spin-Correlation Functions*, Physical Review A **3**, 786.

Appendix A: barcodes for six-partite genuine entangled states

Here we report the 33 different barcodes obtained from randomly generated six-partite genuine entangled states. As usual, barcodes are presented starting from the most frequent to the least frequent one.

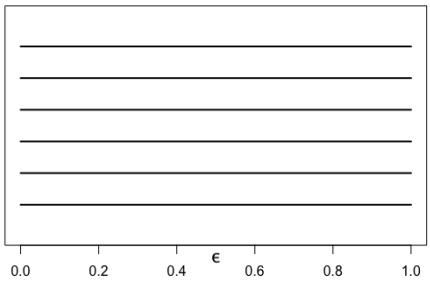

6B1

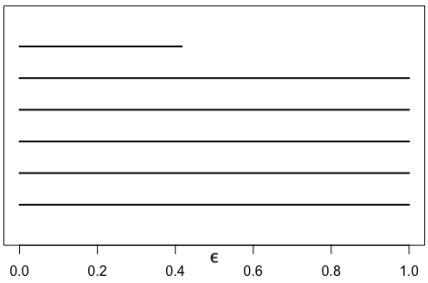

6B2

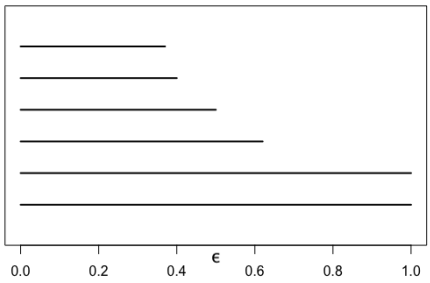

6B3

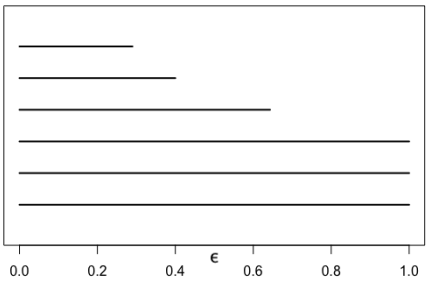

6B4

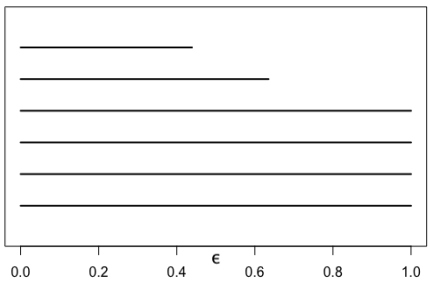

6B5

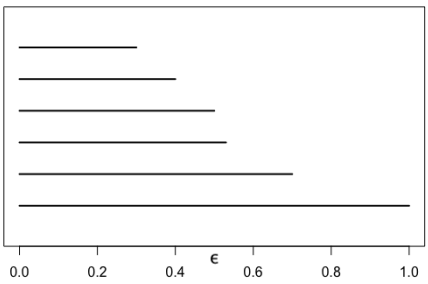

6B6

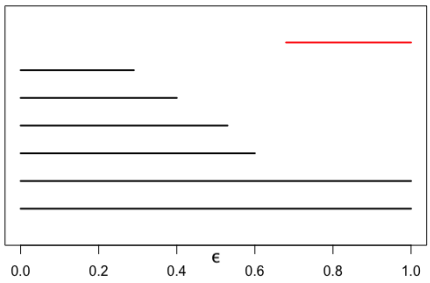

6B7

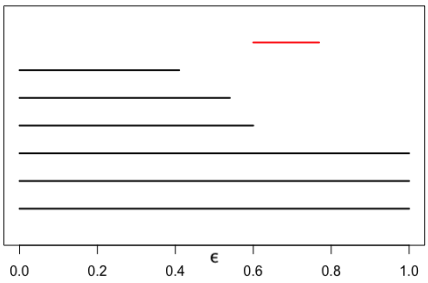

6B8

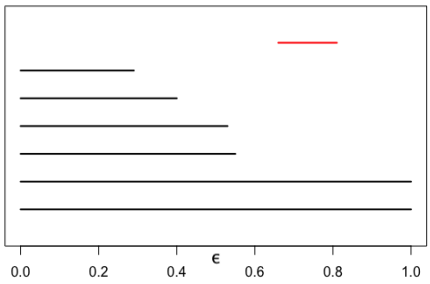

6B9

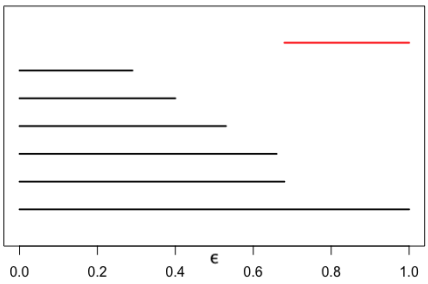

6B10

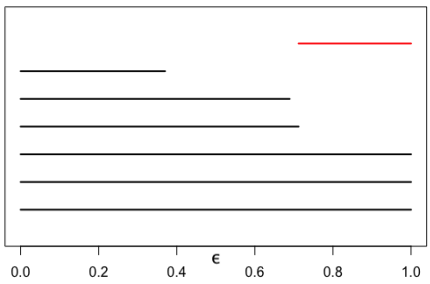

6B11

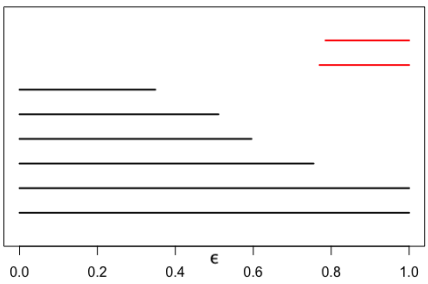

6B12

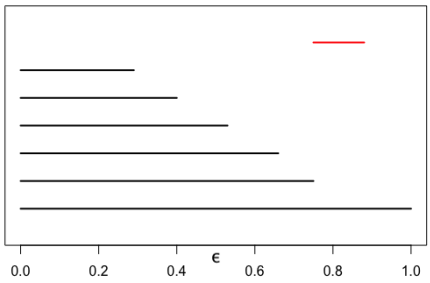

6B13

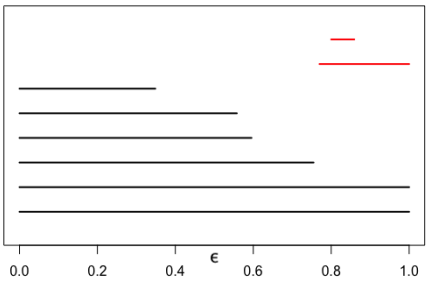

6B14

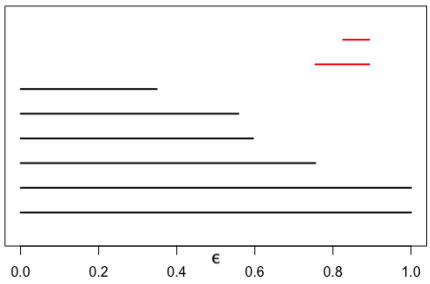

6B15

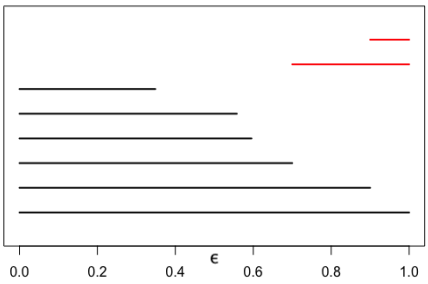

6B16

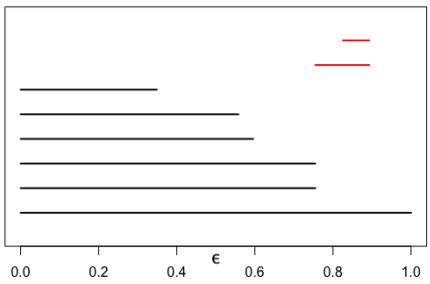

6B17

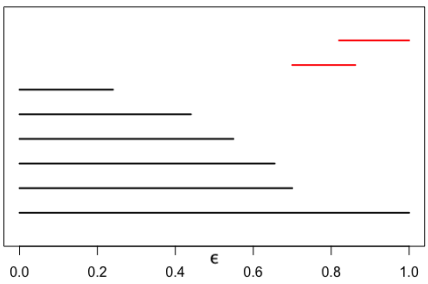

6B18

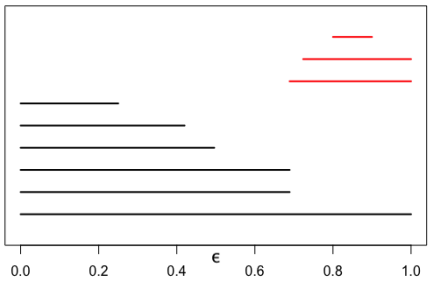

6B19

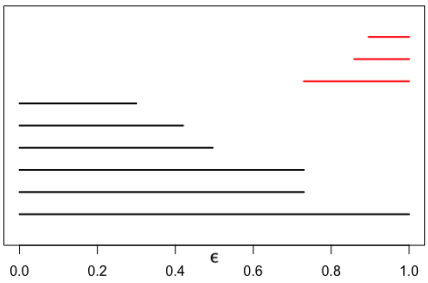

6B20

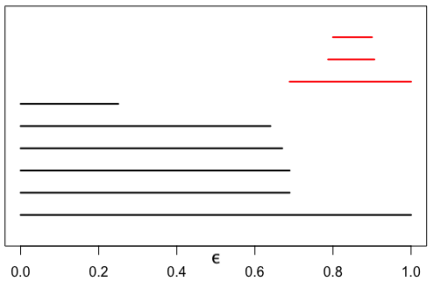

6B21

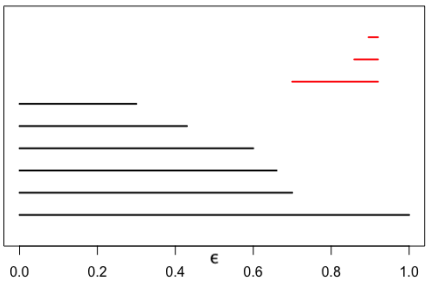

6B22

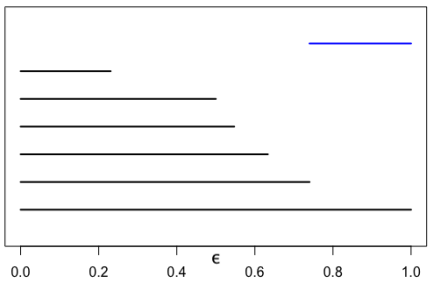

6B23

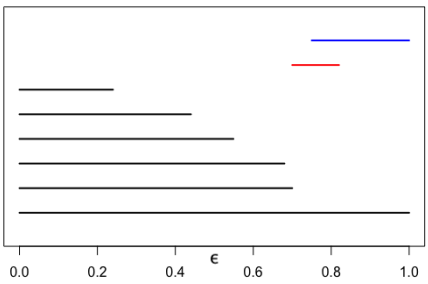

6B24

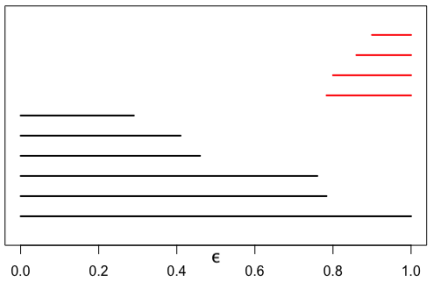

6B25

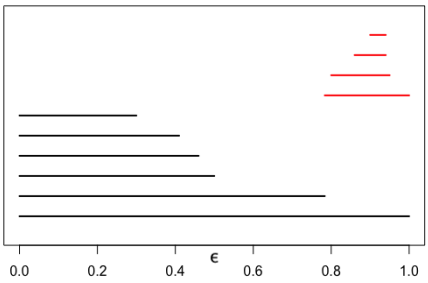

6B26

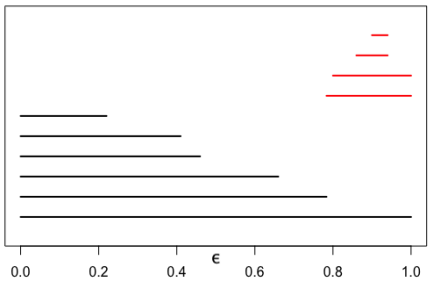

6B27

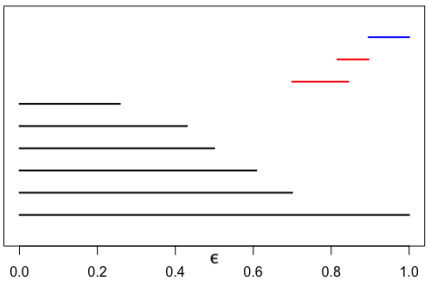

6B28

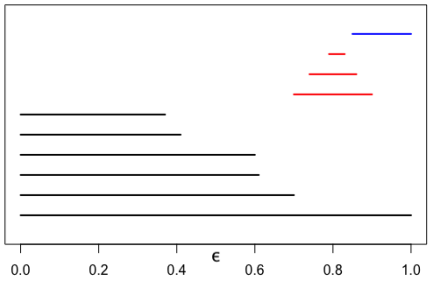

6B29

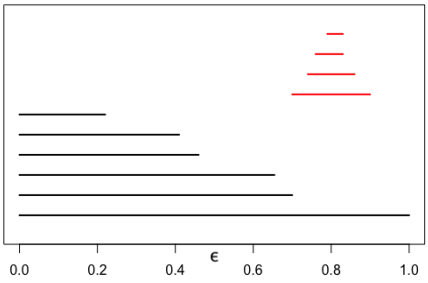

6B30

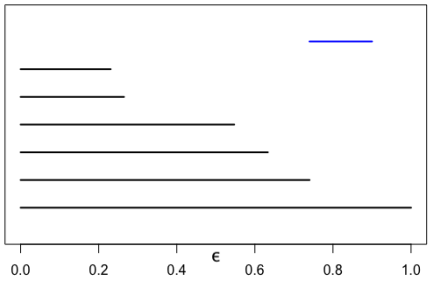

6B31

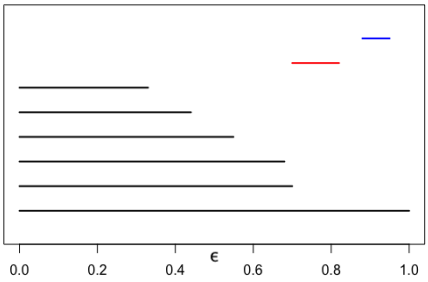

6B32

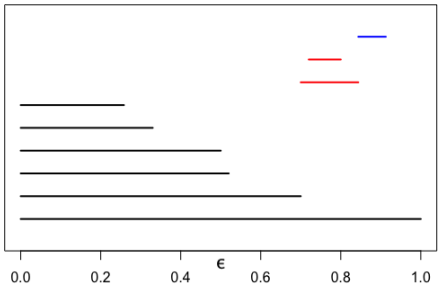

6B33